Efficient Beam-Training Technique for Millimeter-Wave Cellular Communications

Bon Woo Ku, Dae Gen Han, and Yong Soo Cho

In this paper, a beam ID preamble (BIDP) technique, where a beam ID is transmitted in the physical layer, is proposed for efficient beam training in millimeter-wave cellular communication systems. To facilitate beam ID detection in a multicell environment with multiple beams, a BIDP is designed such that a beam ID is mapped onto a Zadoff–Chu sequence in association with its cell ID. By analyzing the correlation property of the BIDP, it is shown that multiple beams can be transmitted simultaneously with the proposed technique with minimal interbeam interference in a multicell environment, where beams have different time delays due to propagation delay or multipath channel delay. Through simulation with a spatial channel model, it is shown that the best beam pairs can be found with a significantly reduced processing time of beam training in the proposed technique.

Keywords: mmWave, cellular system, analog beamforming, beam training, beam ID preamble, Zadoff–Chu sequence.

I. Introduction

Because of rapid growth in both mobile data traffic and the use of smartphones, the millimeter-wave (mmWave) frequency spectrum has been explored for future broadband cellular communication systems [1], [2]. Recently, it has been speculated that multigigabit-per-second data transmission is possible by the use of large spectrum allocation in the mmWave frequency band and steerable beamforming antennas [3]–[5]. Highly directional beamforming antennas are necessary at both the base station (BS) and the mobile station (MS) to compensate for the high attenuation in the mmWave frequency band and to extend the transmission range. With a small wavelength of a mmWave frequency, antenna arrays can be easily installed in the MS.

Currently, an analog beamforming design is preferred over digital beamforming at both the BS and the MS in mmWave communication systems because multiple analog chains at mmWave frequencies are costly, and sampling an analog signal at the gigahertz rate consumes a substantial amount of power [6]. In practice, switched beamforming techniques with a set of predefined angles are being used for transmit–receive (Tx–Rx) beamforming in mmWave communication systems. In switched beamforming systems, the maximum array gain is obtained when Tx and Rx beams are perfectly aligned. A small misalignment between Tx and Rx beams may cause a significant loss in the received power, especially for systems with narrow beams. Therefore, beam training in mmWave communication systems is necessary to find the best beam pair among all possible beam pairs for maximum beamforming efficiency.

The Tx–Rx beamforming technique using the 60 GHz unlicensed spectrum has already been standardized in IEEE

Manuscript received Nov. 7, 2014; revised Aug. 4, 2015; accepted Aug. 12, 2015.

This research was supported by the MSIP (Ministry of Science, ICT and Future Planning), Rep. of Korea, under the ITRC (Information Technology Research Center) support program (IITP-2015-H8501-15-1007) supervised by the IITP (Institute for Information & communications Technology Promotion) and by Chung-Ang University Excellent Student Scholarship.

Bon Woo Ku (gbono1987@naver.com), Dae Gen Han (dae450@naver.com), and Yong Soo Cho (corresponding author, yscho@cau.ac.kr) are with the Department of Electrical Engineering, Chung-Ang University, Seoul, Rep. of Korea.

802.11ad to provide a multigigabit-per-second data rate [7]. However, the IEEE 802.11ad standard is mainly concerned with indoor communication, and does not require handover capability for cellular communication systems. A beam training protocol in a cellular system requires a large amount of training time and network resources because it needs to select a serving BS with the best beam pair after checking the link qualities for all possible beam pairs for all neighbor BSs [8]–[9]. This overhead can be a significant burden for a moving MS because the beam training protocol should be performed periodically for handover or beam tracking.

In this paper, an efficient beam training technique for a mmWave cellular system with analog beams is proposed by transmitting a beam ID preamble (BIDP) in the physical layer. Because the beam ID needs to be detected in a multicell environment with multiple beams, the BIDP is designed such that the beam ID is mapped on a Zadoff–Chu (ZC) sequence in association with its cell ID [10]. Both the beam ID and the cell ID are transmitted on a single BIDP preamble to facilitate joint detection of the beam ID and cell ID. The correlation properties of the BIDP are analyzed in a multicell environment, where there exist different time delays among the beams received from neighbor BSs. It is shown that multiple BIDPs can be transmitted simultaneously in the proposed approach with minimal interbeam interference in a multicell environment, resulting in a significantly reduced processing time for beam training. The performance of the proposed technique is verified by simulation with a spatial channel model (SCM) in a mmWave cellular environment [11]–[13].

II. Preliminary

In the IEEE 802.11ad standard, a two-level scheme composed of a sector level sweep (SLS) phase and a beam refinement protocol (BRP) phase is adopted for beam training [7]. During the SLS phase, a sector level beam sweep is performed, where the best transmit sector beam is selected with a quasi-omni antenna pattern at the receiver. During the BRP phase, refined beam selection is carried out with the receive beam at high resolution to compensate for the imperfection of the quasi-omni antenna pattern. However, in mmWave cellular systems, it is not effective to adopt the quasi-omni antenna pattern for the receive side, because of its large transmission range. Directional beamforming antennas are necessary at both the BS and the MS to maintain a link budget even in the beam training period. The best beam pair in mmWave cellular systems is found by time-division beam switching (TDBS) in the beam training period. In the TDBS scheme, individual Tx beams are transmitted from the BS until all of the Tx beams are transmitted. The Rx beam sweep is performed at the MS for each Tx beam to measure the signal-to-noise ratio (SNR) for every Tx–Rx beam pair. The measurement of SNRs for all possible Tx–Rx beam pairs must be performed for all neighbor BSs to select a serving BS with the best beam pair. The processing time required for beam training in TDBS increases proportionally with the product of the number of Tx beams, number of Rx beams, and number of neighbor BSs. This long processing time will create significant overhead for a moving MS because beam training should be performed periodically for a possible handover or beam tracking. To reduce the processing time for beam training, multiple beams can be transmitted simultaneously during a training period by sending their corresponding Tx-beam IDs in a message type. However, this scheme may increase interbeam interferences in a multicell environment with multiple beams. It also requires MAC-layer processing to decode the received message.

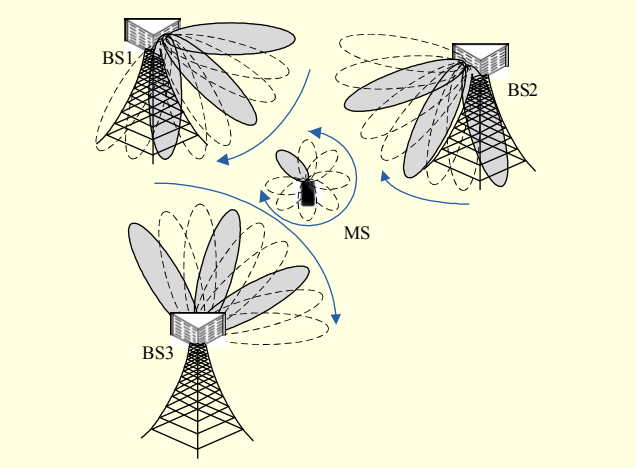

Fig. 1. Example of mmWave cellular system.

In this paper, a BIDP technique where the beam ID is transmitted in the physical layer is described to reduce the processing time for beam training. Figure 1 shows an example of a mmWave cellular system with three BSs and one MS. It is assumed that the switched beamforming technique with a set of predefined angles is used at both the BS and the MS. It is also assumed that the BS has multiple antenna arrays, whereas the MS has only one. Figure 2 shows preamble structures in the proposed technique. Figure 2 shows only the preamble segment, ignoring the data transmission segment in a frame structure. The labels c, a, and b denote the cell ID index, antenna array index, and beam ID index, respectively. The number of Tx beams used at the BS is N_{TX}^{b}; the number of Rx beams at the MS is N_{RX}^{b}; the number of antenna arrays at the BS is $N_{\mathrm{TX}}^{a}(\leq N_{\mathrm{TX}}^{b})$; the number of antenna arrays at the MS is $N_{\mathrm{RX}}^{a}(\leq N_{\mathrm{RX}}^{b})$; and the number of neighbor BSs is N_c. In this paper, it is assumed that $N_{\mathrm{RX}}^{a}=1$. In the proposed technique,

ETRI Journal, Volume 38, Number 1, February 2016
http://dx.doi.org/10.4218/etrij.16.0114.1294

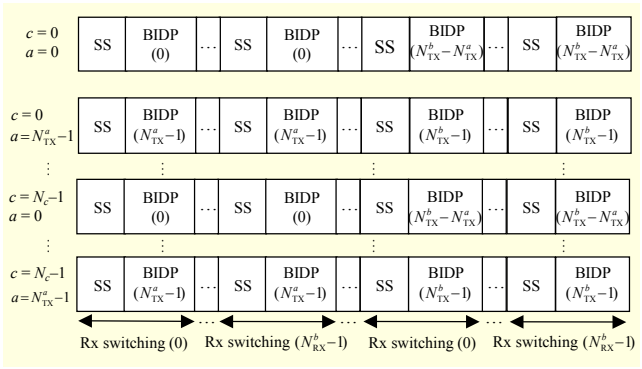

Fig. 2. Preamble structure in proposed technique.

N^a_{TX} beams are simultaneously transmitted from all neighbor BSs (N_c), and Rx beams are swept over in this period. Moreover, N^a_{TX} beams are transmitted repeatedly N^b_{RX} times until one round of the Rx beam sweep is completed. This procedure is repeated N^b_{TX}/N^a_{TX} times by changing Tx beams until all Tx beams are transmitted. If there are N^b_{TX} antenna arrays at the BS, then only one round of an Rx beam sweep is required for beam training because all N^b_{TX} beams are simultaneously transmitted from all neighbor BSs.

In Fig. 2, "SS" represents a synchronization preamble, from which synchronization information and the cell ID are acquired. The beam ID and array ID are acquired from BIDP. In this paper, we assume that synchronization and the cell search procedure have been completed with the SS using the same approach as in LTE systems with synchronization signals (PSS and SSS) [14] or in Mobile WiMAX with preambles. In this paper, we will focus only on the design of BIDP. Note that each BIDP needs to be designed in conjunction with the preceding SS. Because beam IDs and array IDs are detected in a multicell environment with multiple beams, the MS needs to have the capability of identifying its cell ID from the received beam. Therefore, the beam ID and array ID in BIDP need to be designed in conjunction with the cell ID in the SS.

We consider a Tx–Rx beamforming system based on orthogonal frequency-division multiplexing (OFDM). The signal received from the *i*th Rx beam direction at the MS is expressed in the frequency domain as follows:

$$Y_i(k)=\sum_{c=0}^{N_c-1}\sum_{a=0}^{N^a_{TX}-1}G^{c,b(a)}_{TX}G_{RX,i}H^{c,b(a)}_i(k)e^{\frac{-2\pi k\delta^{c,b(a)}_i}{N}}X^{c,b(a)}(k)$$
$$+G_{RX,i}W_i(k)\qquad(k=0,1,\ldots,N-1),\qquad(1)$$

where $G^{c,b(a)}_{TX}$ and $G_{RX,i}$ denote the Tx gain of the *b*th beam transmitted from the *a*th array in the *c*th BS and the Rx gain of the *i*th beam in the MS, respectively. Furthermore, $H^{c,b(a)}_i(k)$ and $\delta^{c,b(a)}_i$ denote the frequency response of the channel between the *b*th beam of the *a*th array in the *c*th BS and the *i*th beam in the MS, and the corresponding symbol timing offset (STO), respectively. Note that the STO is separated from the channel to analyze the effect of STOs on the detection of the beam ID in a multicell environment with multiple beams. Although time synchronization can be achieved on a specific beam pair using the SS, STOs may exist for other Tx–Rx beam pairs in a multicell environment. The carrier frequency offset (CFO) is ignored in this paper. Additionally, $X^{c,b(a)}(k)$ and $W_i(k)$ denote the signal transmitted from the *b*th beam of the *a*th array in the *c*th BS and additive white Gaussian noise (AWGN) received from the *i*th beam in the MS, at the *k*th subcarrier, respectively. The number of subcarriers is denoted by *N*. The *b*th beam of the *a*th array, *b*(*a*), can have a different beam pattern, such as an interleaved type or cluster type, depending on the way in which multiple beams are simultaneously transmitted. In Fig. 1, an interleaved pattern of multiple beams is shown for reduction of interbeam interference.

III. Efficient Beam-Training Technique Using BIDP

A ZC sequence is used for BIDP because it has the property of constant amplitude and zero autocorrelation in both time and frequency domains [10]. Because the beam ID and array ID need to be transmitted in conjunction with the cell ID in BIDP, a large number of IDs need to be mapped to a ZC sequence in an OFDM symbol. In the proposed BIDP, the beam ID, array ID, and cell ID are mapped to a ZC sequence as follows:

$$X^{c,s}(k)\triangleq X^{c,b(a)}(k)=e^{\frac{j\pi r^{(c)}(k+ps)(k+ps+1)}{N_Z}}\qquad(2)$$
$$k=0,1,\ldots,N_Z-1,$$

where

$$s=aN^b_{TX}+b,\quad a=0,1,\ldots,N^a_{TX}-1,\quad b=0,1,\ldots,N^b_{TX}-1,$$
$$\gcd(r,N_Z)=1.$$

Here, $r^{(c)}$ and s denote the root index associated with cell ID c and the index consisting of the beam ID and array ID, respectively. In (2), N_z and p denote a prime number representing the length of the ZC sequence and circular shift spacing in the frequency domain, respectively. Additionally, "gcd" stands for the greatest common divisor. Note that the cell ID is mapped onto the root index of the ZC sequence in the same way as in PSS in LTE systems [14]. The same cell ID used in the preceding SS should be used in BIDP because BIDP needs to be designed in conjunction with the SS. The beam ID and array ID are mapped to the amount of circular shifts of the ZC sequence in the frequency domain.

To find the detection performance of the beam ID, array ID, and cell ID in a multicell environment with multiple beams, we

analyze the correlation properties of BIDP on the receiver side. We assume that BIDPs provided by (2) are simultaneously transmitted from all neighbor BSs with N_{TX}^{b} antenna arrays. Then, the correlation value between the signal received from the *i*th Rx beam at the MS and reference BIDP is provided by

$$
\begin{aligned}
R_i^{\bar{c},\bar{s},\bar{\delta}} &= \sum_{k=0}^{N_z-1} Y_i(k)\left(X^{\bar{c},\bar{s}}(k)e^{\frac{-\mathrm{j}2\pi k\bar{\delta}}{N_Z}}\right)^* \\
&= \sum_{c=0}^{N_c-1}\sum_{s=0}^{N_{\mathrm{TX}}^b-1}\sum_{k=0}^{N_Z-1} G_{\mathrm{TX}}^{c,s}G_{\mathrm{RX},i}H_i^{c,s}(k)X^{c,s}(k)e^{\frac{-\mathrm{j}2\pi k\delta_i^{(c,s)}}{N_Z}}\left(X^{\bar{c},\bar{s}}(k)e^{\frac{-\mathrm{j}2\pi k\bar{\delta}}{N_Z}}\right)^* \\
&= \underbrace{G_{\mathrm{TX}}^{\bar{c},\bar{s}}G_{\mathrm{RX},i}\sum_{k=0}^{N_Z-1}H_i^{\bar{c},\bar{s}}(k)X^{\bar{c},\bar{s}}(k)\left(X^{\bar{c},\bar{s}}(k)\right)^*}_{①} \\
&\quad + \underbrace{\sum_{s=0,s\neq\bar{s}}^{N_{\mathrm{TX}}^b-1} G_{\mathrm{TX}}^{\bar{c},s}G_{\mathrm{RX},i}\sum_{k=0}^{N_Z-1}X^{\bar{c},s}(k)H_i^{\bar{c},s}(k)e^{\frac{-\mathrm{j}2\pi k\delta_i^{(\bar{c},s)}}{N_Z}}\left(X^{\bar{c},\bar{s}}(k)e^{\frac{-\mathrm{j}2\pi k\bar{\delta}}{N_Z}}\right)^*}_{②} \\
&\quad + \underbrace{\sum_{c=0,c\neq\bar{c}}^{N_c-1}\sum_{s=0}^{N_{\mathrm{TX}}^b-1} G_{\mathrm{TX}}^{c,s}G_{\mathrm{RX},i}\sum_{k=0}^{N_Z-1}H_i^{c,s}(k)X^{c,s}(k)e^{\frac{-\mathrm{j}2\pi k\delta_i^{(c,s)}}{N_Z}}\left(X^{\bar{c},\bar{s}}(k)e^{\frac{-\mathrm{j}2\pi k\bar{\delta}}{N_Z}}\right)^*}_{③} \\
&\quad + \underbrace{G_{\mathrm{RX},i}\sum_{k=0}^{N_Z-1}W_i(k)\left(X^{\bar{c},\bar{s}}(k)e^{\frac{-\mathrm{j}2\pi k\bar{\delta}}{N_Z}}\right)^*}_{④},
\end{aligned}
\tag{3}
$$

where $\bar{c},\bar{s}$, and $\bar{\delta}$ denote the reference cell ID, reference index, and reference STO, respectively. Additionally, $\delta_i^{(c,s)}$ denotes the STO between the *s*th beam from the *c*th BS and the *i*th beam in the MS. In (3), ① represents the correlation value when the received beam is matched with the reference BIDP with $\bar{c},\bar{s}$, and $\bar{\delta}$. Label ② represents the interference term caused by autocorrelation when the received beam has the same cell ID as in the reference BIDP ($c = \bar{c}$) but has a different index ($s \neq \bar{s}$). Label ③ represents the interference term caused by cross-correlation when the received beam has a different cell ID ($c \neq \bar{c}$). Label ④ represents the noise term correlated with the reference BIDP. In the following, each term in (3) is analyzed assuming that the channel is nonselective.

Firstly, it is easily observed that the summation term in ① is given by N_z. Secondly, the summation term in ② is expressed as

$$
\begin{aligned}
&\sum_{k=0}^{N_Z-1} X^{\bar{c},s}(k)e^{\frac{-\mathrm{j}2\pi k\delta_i^{(\bar{c},s)}}{N_Z}}\left(X^{\bar{c},\bar{s}}(k)e^{\frac{-\mathrm{j}2\pi k\bar{\delta}}{N_Z}}\right)^* \\
&= \left(X^{\bar{c},\bar{s}}(0)\right)^* X^{\bar{c},s}(0)\sum_{k=0}^{N_Z-1}e^{\frac{\mathrm{j}2\pi k[r^{(\bar{c})}p(s-\bar{s})-(\delta_i^{(\bar{c},s)}-\bar{\delta})]}{N_Z}} \\
&= \begin{cases} \left(X^{\bar{c},\bar{s}}(0)\right)^* X^{\bar{c},s}(0)N_Z & \text{if } \alpha^{(\bar{c},p,s,\bar{s},\delta_i^{(\bar{c},s)},\bar{\delta})} = \mu N_Z, \\ 0 & \text{otherwise,} \end{cases} \\
&\qquad \alpha^{(\bar{c},p,s,\bar{s},\delta_i^{(\bar{c},s)},\bar{\delta})} = r^{(\bar{c})}p(s-\bar{s}) - (\delta_i^{(\bar{c},s)}-\bar{\delta}),
\end{aligned}
\tag{4}
$$

where μ denotes an arbitrary integer value. The correlation value in (4) becomes high when the following condition is satisfied:

$$
r^{(\bar{c})}p(s-\bar{s}) - (\delta_i^{(\bar{c},s)}-\bar{\delta}) = \mu N_Z . \tag{5}
$$

To avoid the condition in (5), the circular shift spacing can be adjusted. The correlation value in (4) becomes high when the circular shift spacing is set to the following value:

$$
p = \frac{\mu N_Z + \Delta\delta}{r^{(\bar{c})}\Delta s}, \qquad p > 0, \tag{6}
$$

$$
\begin{aligned}
&\Delta s = s - \bar{s}, \qquad \Delta\delta = \delta_i^{(c,s)} - \bar{\delta}, \\
&p_{\max} = \left\lfloor \frac{N_Z}{N_s} \right\rfloor, \qquad \mu_{\max} = \left\lceil \frac{r^{(\bar{C})}p_{\max}(N_s-1)+\Delta\delta_{\max}}{N_Z} \right\rceil, \\
&N_s = (N_{\mathrm{TX}}^a - 1)N_{\mathrm{TX}}^b + N_{\mathrm{TX}}^b,
\end{aligned}
$$

where N_s and $\Delta\delta_{\max}$ denote the total number of indices and maximum STO difference between the received beam and reference beam, respectively. Equation (6) is meaningful only when *p* is a non-zero integer value. Therefore, we must select the integer value of *p* that can avoid the condition in (6).

Thirdly, the summation term in ③ can be derived using the property of a Gauss sum [15] as follows:

$$
\begin{aligned}
&\sum_{k=0}^{N_Z-1} X_i^{c,s}(k)e^{\frac{-\mathrm{j}2\pi k\delta_i^{(c,s)}}{N_Z}}\left(X_i^{\bar{c},\bar{s}}(k)e^{\frac{-\mathrm{j}2\pi k\bar{\delta}}{N_Z}}\right)^* \\
&= \sum_{k=0}^{N_Z-1} e^{\frac{\mathrm{j}\pi r^{(c)}(k+ps)(k+ps+1)}{N_Z}}e^{\frac{-\mathrm{j}2\pi k\delta_i^{(c,s)}}{N_Z}}\left(e^{\frac{\mathrm{j}\pi r^{(\bar{c})}(k+\bar{p}\bar{s})(k+\bar{p}\bar{s}+1)}{N_Z}}e^{\frac{-\mathrm{j}2\pi k\bar{\delta}}{N_Z}}\right)^* \\
&= \begin{cases} \sqrt{N_Z}\left(X^{\bar{c},\bar{s}}(0)\right)^* X^{c,s}(0)e^{\frac{-\mathrm{j}\pi\lambda}{N_Z}} & \\ \quad\times\left\langle\frac{\alpha\left|r^{(c)}-r^{(\bar{c})}\right|}{N_Z}\right\rangle\frac{1-j^{N_Z}}{1-j}e^{\frac{-2\pi\left|r^{(c)}-r^{(\bar{c})}\right|\alpha\beta}{N_Z}} & r^{(c)}-r^{(\bar{c})}>0, \\ \sqrt{N_Z}\left(X^{\bar{c},\bar{s}}(0)\right)^* X^{c,s}(0)e^{\frac{-\mathrm{j}\pi\lambda}{N_Z}} & \\ \quad\times\left\langle\frac{\alpha\left|r^{(c)}-r^{(\bar{c})}\right|}{N_Z}\right\rangle\frac{1+j^{N_Z}}{1+j}e^{\frac{-2\pi\left|r^{(c)}-r^{(\bar{c})}\right|\alpha\beta}{N_Z}} & r^{(c)}-r^{(\bar{c})}<0, \end{cases}
\end{aligned}
\tag{7}
$$

where

$$
\begin{aligned}
&\lambda = (ps - \overline{ps} - \delta_i^{(c,s)} + \bar{\delta}) \\
&\quad\times\left(1+(r^{(c)}-r^{(\bar{c})})^{-1}(ps-\overline{ps}-\delta_i^{(c,s)}+\bar{\delta})\right), \\
&\gcd(r^{(c)},N_Z)=1,\ \gcd(r^{(\bar{c})},N_Z)=1,\ \gcd(r^{(c)}-r^{(\bar{c})},N_Z)=1, \\
&\alpha = \frac{N_Z+1}{2},\ \beta = \frac{N_Z-1}{2}.
\end{aligned}
$$

In this equation, $<>$ and $\bar{p}$ denote the Jacobi symbol [15] and reference circular shift spacing in the frequency domain, respectively. Note that the amplitude of (7) is given by $\sqrt{N_z}$.

Then, the upper bound of ③ in terms of the amplitude is expressed using the following triangular inequality:

$$\left| \sum_{c=0,c\neq\bar{c}}^{N_c-1} \sum_{s=0}^{N_{\mathrm{TX}}^b-1} \left\{ G_{\mathrm{TX}}^{c,s} G_{\mathrm{RX},i} H_i^{c,s} \times \sum_{k=0}^{N_Z-1} X^{c,s}(k) e^{\frac{-\mathrm{j}2\pi k\delta_i^{(c,s)}}{N_Z}} \left(X^{\bar{c},\bar{s}}(k) e^{\frac{-\mathrm{j}2\pi k\bar{\delta}}{N_Z}} \right)^* \right\} \right|$$

$$\leq \sum_{c=0,c\neq\bar{c}}^{N_c-1} \sum_{s=0}^{N_{\mathrm{TX}}^b-1} \left\{ \left| G_{\mathrm{TX}}^{c,s} G_{\mathrm{RX},i} H_i^{c,s} \right| \times \left| \sum_{k=0}^{N_Z-1} X^{c,s}(k) e^{\frac{-\mathrm{j}2\pi k\delta_i^{(c,s)}}{N_Z}} \left(X^{\bar{c},\bar{s}}(k) e^{\frac{-\mathrm{j}2\pi k\bar{\delta}}{N_Z}} \right)^* \right| \right\}$$

$$= \sqrt{N_Z} \sum_{c=0,c\neq\bar{c}}^{N_c-1} \sum_{s=0}^{N_{\mathrm{TX}}^b-1} \left| G_{\mathrm{TX}}^{c,s} G_{\mathrm{RX},i} H_i^{c,s} \right|, \quad (8)$$

where

$$\left| \sum_{k=0}^{N_Z-1} X^{c,s}(k) e^{\frac{-\mathrm{j}2\pi k\delta_i^{(c,s)}}{N_Z}} \left(X^{\bar{c},\bar{s}}(k) e^{\frac{-\mathrm{j}2\pi k\bar{\delta}}{N_Z}} \right)^* \right| = \sqrt{N_Z}.$$

Note that the interference term caused by cross-correlation is bounded by the multiplication of $\sqrt{N_z}$ and summation term on the right-hand side of (8). However, most of the channel gains in the summation term in (8) are small because most of the Tx beams from other BSs and the Rx beam in the MS are not aligned in ③. On the other hand, ① has a large value because it is given by the multiplication of N_z and the channel gain. In this case, the channel gain is usually high because the Tx and Rx beams are aligned. For example, the ratio between $\sqrt{N_z}$ and N_z is 3% when $N_z = 1{,}021$. That is, the interference term caused by the beam transmitted from neighbor BSs is relatively small compared with the signal from the target beam. If we select the value of p avoiding the condition in (6), then the interference term caused by other beams in the same cell can also be ignored. Therefore, the best beam pair ID can be detected by finding the Tx beam that produces the maximum correlation value as follows:

$$[\hat{i},\hat{c},\hat{s},\hat{\delta}] = \arg\max_{i,c,s,\delta} \left\{ R_i^{\bar{c},\bar{s},\bar{\delta}} \right\}, \quad (9)$$

$$[\hat{a}] = \left\lfloor \frac{\hat{s}}{N_{\mathrm{TX}}^b} \right\rfloor,$$

$$[\hat{b}] = \mathrm{mod}(\hat{s}, N_{\mathrm{TX}}^b).$$

Although the beam training technique is described assuming that one antenna array is available at the MS in this paper, the proposed BIDP technique can be easily extended to the case with multiple antennas at the MS. In this case, secondary and tertiary beam pairs need to be detected in addition to the best beam pair provided by (9) to obtain an additional diversity gain or multiplexing gain. Additionally, the time of one round of an Rx beam sweep can be further reduced by simultaneously sweeping Rx beams in the beam training period.

IV. Simulation

In this section, the performance of the proposed BIDP technique is evaluated by computer simulation using a simple model of a mmWave cellular system. It is assumed that an MS is located at the cell boundary among three cells, as shown in Fig. 3. The carrier frequency, bandwidth, and FFT size are set to 28 GHz, 500 MHz, and 2,048, respectively [16]. The number of antenna elements in each array is 16 for a uniform linear array (ULA) in the BS and for a uniform circular array (UCA) in the MS. Additionally, $N_{\mathrm{TX}}^a = N_{\mathrm{TX}}^b = 12$, and $N_{\mathrm{RX}}^a = 1$. The length of the ZC sequence, N_z, is set to 1,021. Cell IDs for the three BSs are mapped to root indices of 54, 59, and 63. It is assumed that the channel between each BS to the MS experiences Rician fading, consisting of one line-of-sight (LOS) path and one non-line-of-sight (NLOS) path [1], [4], [5], [17], and [18]. For simulation, the SCM is used with a k-factor equal to 6 dB [11]. The number of rays in the NLOS path is set to 20. For example, the indices for the LOS path between BS2 and the MS are 52 ($a = 4$, $b = 4$) for the Tx beam and 8 for the Rx beam. For the NLOS path, they are 104 ($a = 8$, $b = 8$) for the Tx beam and 7 for the Rx beam. The SNR in the MS is set to 10 dB.

In Fig. 4, the effect of STO on autocorrelation is examined. In this simulation, the cell ID is mapped to root index 59. It is

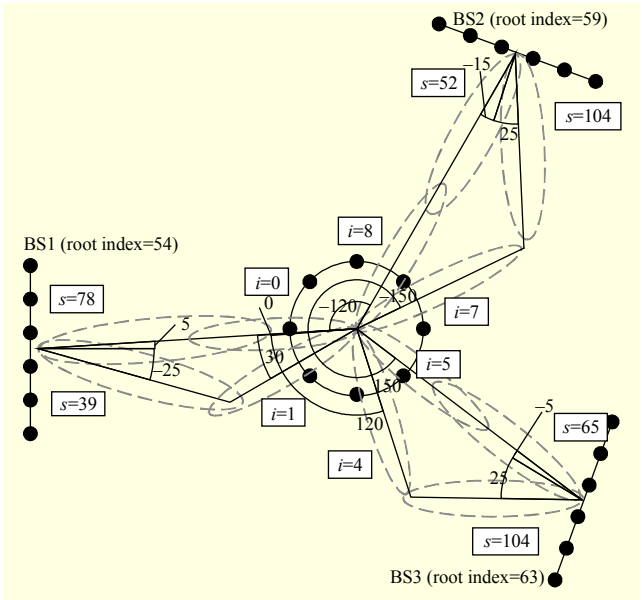

Fig. 3. Simulation setup for simple model of mmWave cellular system.

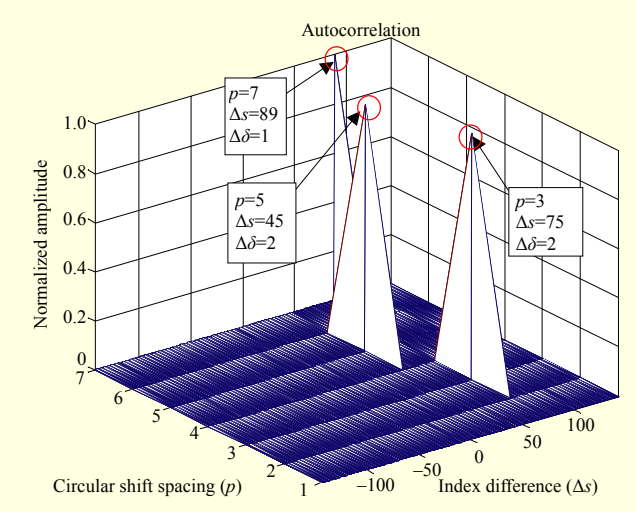

Fig. 4. Autocorrelation values when BIDP is used.

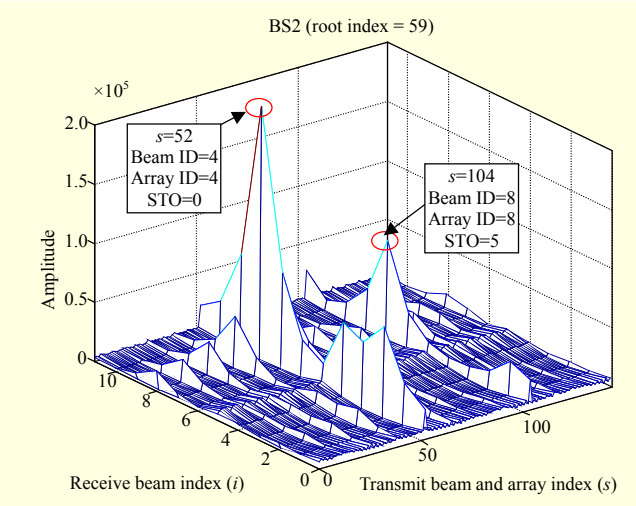

Fig. 5. Correlation values when BIDP is used.

assumed that the value of STO is between one and three, and the index difference ranges from –143 to 143 (excluding the case of $\Delta s = 0$). With these parameters, we can calculate the value (p) of the circular shift spacing satisfying (6); that is, three when $\Delta s = 75$, five when $\Delta s = 45$, and seven when $\Delta s = 89$. For example, the autocorrelation has a high peak at $p = 5$ when $\Delta\delta = 2$, $\mu = 13$, and $\Delta s = 45$, as shown in Fig. 4. Therefore, the values of circular shift spacing satisfying (6) should not be selected when the BIDP is designed. To avoid the interbeam interference caused by STOs, the values of one, one, and two are selected for circular shift spacing in the following simulation because the root indices for cell IDs are set to 54, 59, and 63, respectively.

Figure 5 shows the correlation value between the reference BIDP (root index 59 (BS2)) and the signal received from the MS in Fig. 3. The STO is randomly generated with a value between zero and six. This figure shows that there are peaks at the values of the Tx indices (Tx beam ID and array ID) and Rx indices associated with the LOS and NLOS paths. Peaks exist at $s = 52$ and $i = 8$, corresponding to the LOS path, and at $s = 104$ and $i = 7$, corresponding to the NLOS path. Note that there are peaks only when δ is matched to STO. There are small peaks caused by sidelobes in the beam patterns of the Tx and Rx arrays. Figure 5 shows that there is no interbeam interference caused by STOs with an appropriate selection of p, and the interference term caused by cross-correlations given in (8) is very small.

Figure 6 shows the BER performance when the best beam pairs (LOS) are selected by the proposed BIDP technique. The same channel model is used for the simulation (SCM with a k-factor equal to 6 dB). Simulations are performed for four different cases (1 × 1, 16 × 1, 1 × 16, and 16 × 16), where the first and second terms denote the number of antenna elements in the

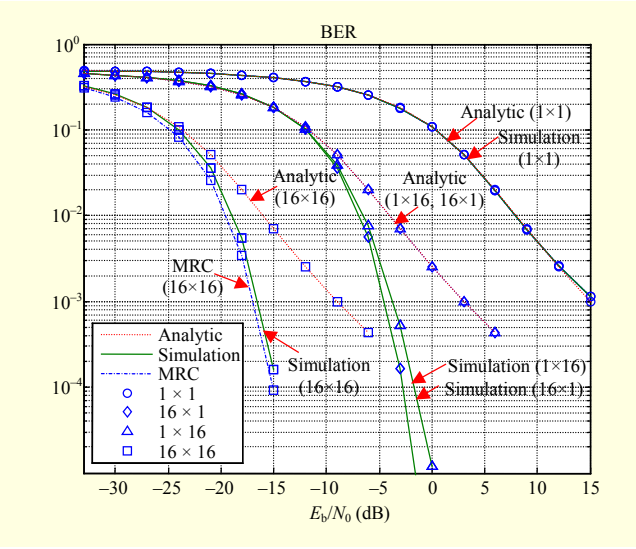

Fig. 6. BER performance when proposed BIDP technique is used.

Tx and Rx sides, respectively. Analytic curves for a Rician fading channel with a k-factor equal to 6 dB are inserted for reference. QPSK modulation is used. This figure shows that the simulation results are the same as the analytic results for the omni case (1 × 1). An array gain of 12 dB (24 dB) can be obtained in the analytic case when an antenna array is employed at the Tx side or Rx side (Tx and Rx sides). Note that the simulation results are better than the analytic results when an antenna array is employed. This is because the SCM channel can be approximated as an AWGN channel in the simulation when beamforming is performed in the direction of the LOS path, whereas only the array gain is considered in the analytic results (Rician fading channel). When two antenna arrays are available at the MS, an additional MRC gain of 0.5 dB is obtained by combining the LOS and NLOS paths.

Table 1. Parameters for performance comparison.

Parameter	Value
TX power (dBm)	35.00
Carrier frequency (GHz)	28.00
Propagation loss (dB)	$32.4 + 20\log(f) + 20\log(d)$
Other losses	20.00
Bandwidth (MHz)	500
Thermal PSD (dBm/Hz)	–174

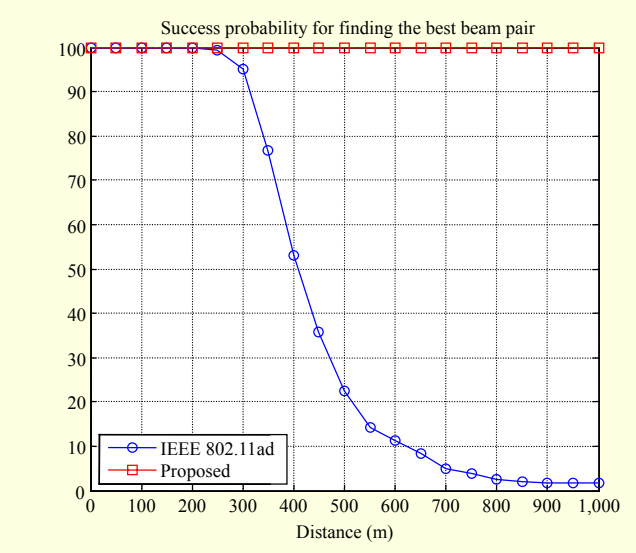

Fig. 7. Success probability of finding best beam pair.

Next, the proposed technique is compared with the IEEE 802.11ad scheme in terms of the success probability in finding the best beam pair. To focus on beam-searching probability, it is assumed that cell ID detection and synchronization are perfect. In the IEEE 802.11ad scheme, it is assumed that there is no error in the feedback loop where the beam ID detected from the receiver side is sent back to the transmitter side. Table 1 shows parameters used for the performance comparison. Other parameters used in the proposed technique are from [19].

Here, f and d in the propagation loss denote the carrier frequency (GHz) and distance (m), respectively. Other losses include the losses caused by cables, penetration, and diffraction. The number of Tx antenna elements and Rx antenna elements is set to eight in each case. Figure 7 shows the success probability of finding the best beam pair when the distance between transmitter and receiver increases. From Fig. 7, one can see that the success probability of finding the best beam pair in the IEEE 802.11ad scheme decreases starting from 250 m, while the success probability of the proposed technique is maintained up to 1 km.

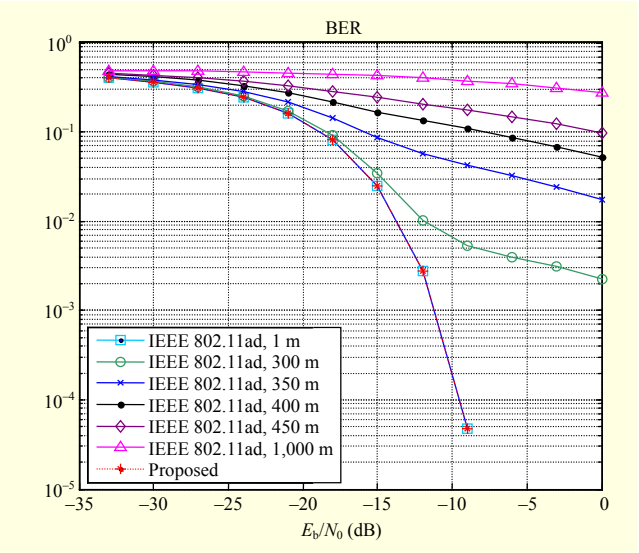

Fig. 8. BER performance of two different techniques in data transmission period.

Figure 8 shows BER performances of two different techniques (the IEEE 802.11ad scheme and the proposed technique) for a given data transmission period, with the beam pair selected during the beam-training period. From this figure, one can see that the BER performance of the proposed technique is not degraded through 1 km. However, the BER performance of the IEEE 802.11ad scheme degrades significantly as the distance increases. The BER performance of the IEEE 802.11ad scheme is almost the same as that of the proposed technique when the distance is small (1 m). However, the IEEE 802.11ad scheme experiences significant performance degradation at a distance of 300 m, although the success probability of finding the best beam pair at that distance is approximately 95%.

The reason that the BER of the IEEE 802.11ad scheme degrades as the distance increases is that a mismatch between the discoverable coverage area and the actual supportable coverage area occurs [19]. In the IEEE 802.11ad scheme, the discoverable coverage area will be much smaller than the actual supportable coverage area. Note that a quasi-omni beam pattern is used at the receiver side in the SLS phase to reduce complexity, resulting in a reduction of discoverable coverage area. After finishing the beam-training period, beams will be formed at both the Tx and Rx side during the data transmission period, resulting in an increase in supportable coverage area. However, the direction of the beams in the data transmission period may not be optimal, because the beam IDs are selected with an omni beam pattern in the SLS phase. On the other hand, in the proposed technique, directional beam-forming antennas are used at both the Tx and Rx side to maintain a link budget even during the beam-training period.

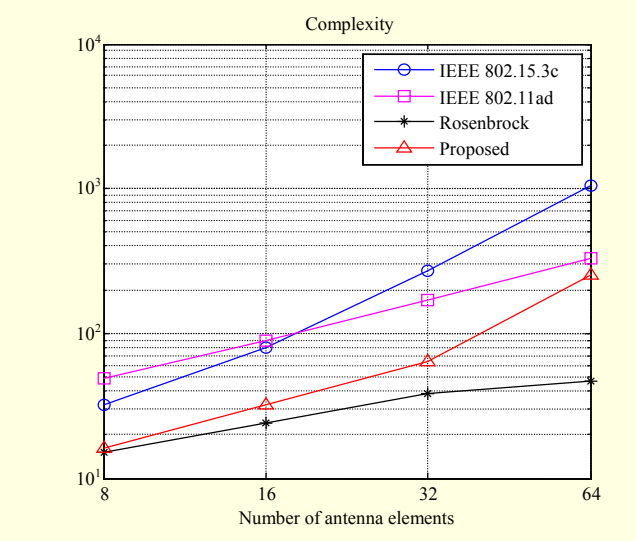

Fig. 9. Complexity comparison among four beam searching schemes.

Table 2. Processing time required for beam training when conventional TDBS and proposed BIDP techniques are used.

	TDBS	BIDP	
Processing time	$T_{SS} \times N_{RX}^{b} \times N_{TX}^{b} \times N_{BS}$	$(T_{SS} + T_{BIDP}) \times N_{RX}^{b} \times (N_{TX}^{b} / N_{TX}^{a})$	
Example	3,594 μs	$N_{TX}^{a} = 1$	1,797 μs
		$N_{TX}^{a} = 6$	300 μs
		$N_{TX}^{a} = 12$	150 μs

Next, the complexity required for the proposed beam training technique is compared with those for conventional beam searching schemes (IEEE 802.15.3c, IEEE 802.11ad, and the beam searching scheme in [20]). The beam-searching scheme in [20] is based on the Rosenbrock algorithm using the concept of small-region dividing and conquering. To compare complexities required for the four beam searching schemes, a single-cell environment is considered in the proposed technique. Figure 9 shows the complexity comparison among the four beam searching schemes when the number of antenna elements varies. Here, it is assumed that the number of Tx sectors and number of Rx sectors in the conventional schemes is set to four and four, respectively. The number of Tx antenna elements is set to be the same as the number of Rx antenna elements.

From Fig. 9, one can see that the complexity of the IEEE 802.15.3c scheme increases rapidly as the number of antenna elements increases. Note that the complexity of the IEEE 802.15.3c scheme increases in $O(N^2)$. The complexities of both the IEEE 802.11ad scheme and the proposed technique are lower than those of the IEEE 802.15.3c scheme, because they are in $O(N)$. The complexity of the beam training scheme in [20] (Rosenbrock direct search) is lowest because it is in $O(\log_2 N)$. However, the conventional beam searching schemes cannot be used in a multicell environment, because they cannot determine the BS that has transmitted the beam.

In Table 2, the processing time required for beam training in the conventional TDBS and proposed BIDP techniques is compared. It is assumed that the number of neighbor BSs (N_{BS}) is three, and the number of antenna arrays at the MS is one. Variables T_{SS} and T_{BIDP} represent the length of the SS and BIDP symbols, respectively. It is also assumed that T_{SS} is equal to two symbol lengths (as in LTE), and T_{BIDP} is equal to one symbol length (because the BIDP is composed of one OFDM symbol). This table shows that the BIDP technique requires smaller processing time than the TDBS technique, even though one additional symbol is used for the BIDP technique. In the BIDP technique, the processing time required for beam training decreases in proportion to the number of Tx antenna arrays. For example, the BIDP technique with six antenna arrays requires only 8% of the processing time using the TDBS technique. As the number of neighbor BSs increases, the processing time for beam training increases linearly in the TDBS technique, whereas it does not change in the BIDP technique.

V. Conclusion

In this paper, an efficient beam training technique for a mmWave cellular system with analog beams was proposed by transmitting the beam ID in the physical layer. It was shown by simulation with SCM that multiple BIDPs can be simultaneously transmitted in the proposed technique with minimal interbeam interference in a multicell environment where there exist different STOs among the beams. It was also shown that the proposed BIDP technique can significantly reduce the processing time of beam training in a multicell environment, especially when multiple antenna arrays are available at the BS. Although the proposed technique was described for a system with analog beams at both the BS and the MS, it can be readily applied to a system with a digital beamformer at the BS and an analog beamformer at the MS because multiple beams can be simultaneously transmitted from the BS with a digital beamformer using only one antenna array.

References

[1] S. Rangan, T.S. Rappaport, and E. Erkip, "Millimeter-Wave Cellular Wireless Networks: Potentials and Challenges," *Proc. IEEE*, vol. 102, no. 3, Mar. 2014. pp. 366–385.

[2] T.S. Rappaport et al., "Millimeter Wave Mobile Communications for 5G Cellular: It Will Work!," *IEEE Access*, vol. 1, 2013, pp. 335–349.
[3] T.S. Rappaport et al., "Broadband Millimeter-Wave Propagation Measurements and Models Using Adaptive-Beam Antennas for Outdoor Urban Cellular Communications," *IEEE Trans. Antennas Propag.*, vol. 61, no. 4, Apr. 2013, pp. 1850–1859.
[4] M.R. Akdeniz et al., "Millimeter Wave Channel Modeling and Cellular Capacity Evaluation," *IEEE J. Sel. Areas Commun.*, vol. 32, no. 6, June 2014, pp. 1164–1179.
[5] Z. Muhi-Eldeen, L.P. Ivrissimtzis, and M. Al-Nuaimi, "Modeling and Measurements of Millimeter Wavelength Propagation in Urban Environments, *IET Microw. Antennas Propag.*, vol. 4, no. 9, Sept. 2010, pp. 1300–1309.
[6] B. Li et al., "Efficient Beamforming Training for 60-GHz Millimeter-wave Communications: A Novel Numerical Optimization Framework," *IEEE Trans. Veh. Technol.*, vol. 63, no. 2, Feb. 2014, pp. 703–717.
[7] IEEE 802.11ad Standard, *Part 11: Wireless LAN Medium Access Contr. (MAC) and Physical Layer (PHY) Specification*, Oct. 2012.
[8] Y. Shen, T. Luo, and Z. Moe, "Neighboring Cell Search for LTE Systems," *IEEE Trans. Wireless Commun.*, vol. 11, no. 3, Mar. 2012, pp. 908–919.
[9] Y.H. Ko et al., "2-D DoA Estimation with Cell Searching for a Mobile Relay Station with Uniform Circular Array," *IEEE Trans. Commun.*, vol. 58, no. 10, Oct. 2010, pp. 2805–2809.
[10] S. Beyme and C. Leung, "Efficient Computation of DFT of Zadoff-Chu Sequences," *Electron. Lett.*, vol. 45, no. 9, Apr. 2009, pp. 461–463.
[11] 3GPP TR 25.996, "Spatial Channel Model for Multiple Input Multiple Output Simulations," Tech. Rep., Release 11, Sept. 2012.
[12] M. Jiang et al., "3D Channel Model Extensions and Characteristics Study for Future Wireless System," *IEEE Int. Symp. Pers. Indoor Mobile Radio Commun.*, London, UK, Sept. 8–11, 2013, pp 41–46.
[13] 3GPP TR 36.873 v1.2.0, "Study on 3D Channel Model for LTE," Tech. Rep., Release 12, 2013.
[14] S. Sesia, I. Toufik, and M. Baker, "*LTE - The UMTS Long Term Evolution: From Theory to Practice*," Chichester, UK: John Wiley and Sons, 2012, pp. 151–163.
[15] B.C. Berndt, R.J. Evans, and K.S. Williams, "*Gauss and Jacobi Sums*," New York, USA: John Wiley and Sons, 1998, pp. 15–26.
[16] Z. Pi and F. Khan, "An Introduction to Millimeter-Wave Mobile Broadband Systems," *IEEE Commun. Mag.*, vol. 49, no. 6, June 2011, pp. 101–107.
[17] M. Cudak et al., "Moving towards mmWave-Based Beyond-4G (B-4G) Technology," *IEEE Veh. Technol. Conf.*, Dresden, Germany, June 2–5, 2013, pp 1–5.
[18] I. Sarris and A.R. Nix, "Ricean K-Factor Measurements in a Home and an Office Environment in the 60 GHz Band," *Mobile Wireless Commun. Summit*, Budapest, Hungary, July 1–5, 2007, pp. 1–5.
[19] Q. Li et al., "Anchor-Booster Based Heterogeneous Networks with mmWave Capable Booster Cells," *IEEE Globecom Workshop*, Atlanta, GA, USA, Dec. 9–13, 2013, pp. 93–98.
[20] B. Li et al., "On the Efficient Beam-Forming Training for 60 GHz Wireless Personal Area Networks," *IEEE Trans. Wireless Commun.*, vol. 12, no. 2, Feb. 2013, pp. 504–515.

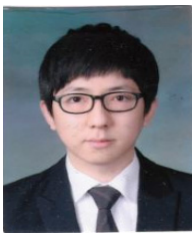

Bon Woo Ku received his BS and MS degrees in electronics engineering from Chung-Ang University, Seoul, Rep. of Korea, in 2013 and 2015, respectively. He is currently a research engineer at Hyundai Mobis, Yongin, Rep. of Korea. His research interest is vehicular communication, especially V2X.

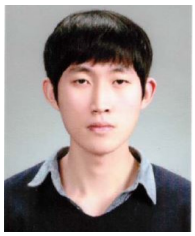

Dae Gen Han received his BS degree in electronics engineering from Chung-Ang University, Seoul, Rep. of Korea, in 2014. He is currently working toward his MS degree in electronics engineering at Chung-Ang University. His research interest is in the area of wireless communication, especially MIMO-OFDM.

Yong Soo Cho received his BS degree in electronics engineering from Chung-Ang University, Seoul, Rep. of Korea; his MS degree in electronics engineering from Yonsei University, Seoul, Rep. of Korea; and his PhD degree in electrical and computer engineering from the University of Texas at Austin, USA, in 1984, 1987, and 1991, respectively. During 1984, he was a research engineer at Goldstar Electrical Company, Osan, Rep. of Korea. In 1992, he joined Chung-Ang University, where he is currently a professor with the School of Electrical and Electronic Engineering. His research interest is in the area of wireless communication, especially MIMO-OFDM.